Photophysical Details and O$_2$-Sensing Analysis of a Eu(III) Complex in Polymer Composite Nanofibers Prepared by Electrospinning

Chunguo Cui[1†], Lina Song[2†], Chao Li[3], Tiantian Lin[3] and Kaiyao Shi[3*]

[1]Department of Breast Surgery, China–Japan Union Hospital of Jilin University, Changchun, China, [2]Department of Laboratory, 15189 Accredited Laboratory, Jilin Province Drug Resistance Monitoring Center, China-Japan Union Hospital of Jilin University, Changchun, China, [3]Provincial Key Laboratory for Gene Diagnosis of Cardiovascular Disease, Jilin Provincial Engineering Laboratory for Endothelial Function and Genetic Diagnosis, Department of Cardiology, China-Japan Union Hospital of Jilin University, Changchun, China

An as-synthesized Eu(III) complex, denoted as Eu(N-DPNQ)(TTD)$_3$, was prepared and characterized, and the antenna mechanism between these ligands and central metal emitter was studied. Here DPNQ means 10-ethyl-10H-indolo [2′,3′:5,6]pyrazino[2,3-f] [1,10]phenanthroline and TTD is 4,4,4-trifluoro-1-(thiophen-2-yl)butane-1,3-dione. We find that Eu(N-DPNQ)(TTD)$_3$ emission intensity dependents on oxygen concentration, and O$_2$-sensing skill of Eu(N-DPNQ)(TTD)$_3$ in polymer composite nanofibers of poly (vinylpyrrolidone) (PVP) prepared by electrospinning is investigated. Results reveal that the emission quenching of Eu(N-DPNQ)(TTD)$_3$ is caused by the ground state (triplet) oxygen quenching on antenna ligands triplet state. The Eu(N-DPNQ)(TTD)$_3$ doped composite nanofiber with a loading level of 6 wt% exhibits the best result with sensitivity of 2.43 and response time of 10 s, along with linear response.

Keywords: Eu(III) complex, oxygen-sensing, electrospinning, emission quenching, polymer host

INTRODUCTION

Rare earth metal compounds are attractive ones, showing wide applications in laser and luminescence and serving as probes in porous and bio-active materials. Their advantages include efficient emission, long-lived fluorescence and sharp emission peaks (Sun et al., 2002; Xu et al., 2002; Gunnlaugsson et al., 2003; Sun et al., 2003; Gunnlaugsson et al., 2004; Nakamura et al., 2007; Ai et al., 2009; Zhang et al., 2009; Park et al., 2010; Zhang et al., 2010). Very recently, the emission features of Eu(III) emitters grafted on a solid host have been systematically investigated (Xu et al., 2002; Li et al., 2006; Li and Yan, 2008; Yan and Wang, 2008; Li Kong et al., 2009). Some Eu(III) complexes have been demonstrated as optical O$_2$-sensing probes (Amao et al., 2000a; Amao et al., 2000b; Zuo et al., 2010).

Long nanofibers have found their potential applications such as reinforcement, filters, textiles, catalysis and medicine. Electrospinning is a fascinating method for preparation of fibers at nanometer level, and has been already applied in many technological areas (Huang et al., 2003). As a fibers drawing technique, electrospinning is finished *via* the drawing of polymer solutions and melts (Zhang et al., 2007a). The fiber shape and morphology are controlled by many parameters, such as polymer nature (molecular weight and its distribution, glass temperature and compatibility), physical characters of the precursor solution (doping level, conductivity, tension and so on), solvent partial pressure, field strength, and environmental humidity. It is particularly fascinating that the polymers can be decorated

SCHEME 1 | Synthetic routes for N-DPNQ and Eu (N-DPNQ) (TTD)$_3$.
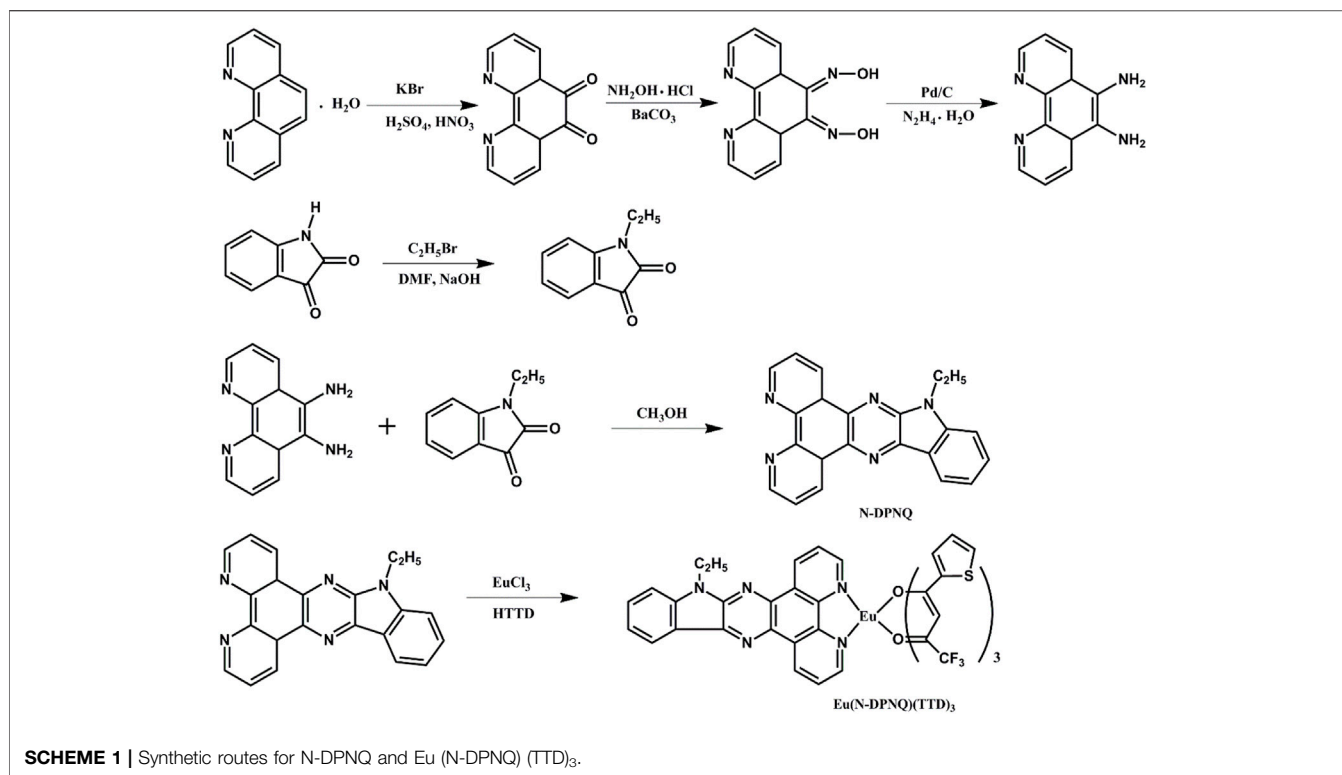
and adjusted by various dopants such as luminescent phosphors and dyes by electrospinning (Greiner and Wendorff, 2007). Therefore, several functionalized composite nanofibers have been proposed, along with their practical application (Wang et al., 2002; Baldé et al., 2008; Dodiuk-kenig et al., 2008; Liu et al., 2008; Tan et al., 2008; Takahashi et al., 2009; Wang F. et al., 2009; Wang W. et al., 2009; Wang Y. et al., 2009). One of the most important application of composite nanofibers is chemical sensing or biosensing profiting from their vast surface area, which may lead to super-sensitive and instant response during sensing process.

In this article, a novel oxygen-sensing Eu(III) probe of Eu(N-DPNQ)(TTD)$_3$ is synthesized, and incorporated into polymer composite nanofibers using electrospinning method. Here, a polymer PVP is selected as the supporting host for this oxygen-sensing probe, owing to its virtues of good mechanical strength, stable physical property and good compatibility with various dopants (Wang et al., 2002; Wang W. et al., 2009; Wang Y. et al., 2009). The vast surface area and the uniform dispersal of the resulting composite samples accelerate oxygen diffusion, leading to sensitivity improvement and response time decrease of oxygen sensor. O$_2$-sensing parameters of the composite nanofibers upon three loading contents are compared and investigated, as well as luminescence quenching mechanism.

EXPERIMENTAL

Materials and Apparatus

PVP (*molecular weight* ≈ 60000) was purchased from Tanggu Chemicals Corporation (China). Eu$_2$O$_3$ and 1, 10-

Phenanthroline were bought *via* Shanghai Chemical Ltd. (China). Isatin and Pd/C were ordered from Aldrich Chemical Ltd. N, N-dimethylformamide (DMF), bromoethane, EtOH, 1, 2-dichloroethane and concentrated HCl were supplied by Tianjin Chemicals Corporation. Elemental analysis was obtained using a Vario Element Analyzer. ^{1}H NMR experiment was deployed on a Bruker-DPX-300 spectrometer. IR experiment was finished by a Magna560 spectrometer. Thermogravimetric experiment was performed on a Perkin-Elmer thermal analyzer. Phosphorescence spectrum was determined at liquid N$_2$ temperature by FLS 920 spectrometer.

The fiber size and morphology were obtained using a Hitachi S-4800 microscopy. Absorption experiment was done on a Cary 500 spectrometer. Emission experiment was done by a Hitachi F-4500 spectrometer. For Stern-Volmer plots experiment, O$_2$ and N$_2$ were controlled by gas flowmeters and mixed in a quartz chamber.

Synthesis of N-DPNQ and its Complex

Related synthetic schemes for N-DPNQ and its europium complex are summarized as **Scheme 1**.

N-DPNQ: the related two starting compounds were obtained following reported methods (Bolger et al., 1996; Bian et al., 2002). N-DPNQ was synthesized by modification of the literature method (Bodige and MacDonnell, 1997). The detailed synthetic routes were described as follows: (0.756 g, 3.6 mmol) 1, 10-phenanthroline-5, 6-diamine was added into 80 ml of methanol under, and (0.525g, 3 mmol) 1-ethylindoline-2,3-dione was added to the solution. This solution was refluxed for 8 h. After cooling the mixture, solid product was filtered
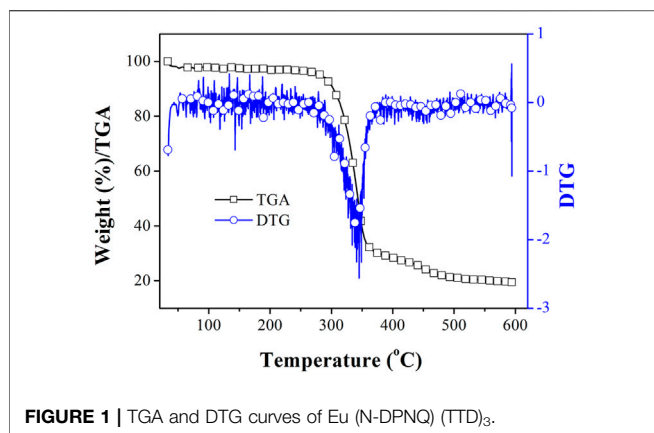
FIGURE 1 | TGA and DTG curves of Eu (N-DPNQ) (TTD)₃.

off and washed by EtOH. The solid powder wasrecrystallized from methanol. ^{1}H NMR(CDCl₃, 500 MHz) δ [ppm]: 9.22 (d, 1H), 9.13 (d, 1H), 9.05 (d, 1H), 8.52 (d, 1H), 7.66–7.72 (m, 2H), 7.57 (d, 1H), 7.34 (d, 1H), 7.28 (s, 2H), 4.34 (t, 2H), and 1.34 (t, 3H). ^{13}C NMR δ [ppm]: 150.2, 147.7, 145.8, 139.9, 138.8, 137.7, 137.0, 134.9, 127.8, 124.2, 123.0, 121.5, 120.2, 109.8, 39.4, 14.2. Calculated for $C_{22}H_{15}N_5$: 349.1, MS Found: 349.0 [M]$^{+}$.

Eu(N-DPNQ)(TTD)₃. This compound was prepared in accordance with a published method (Bauer et al., 1964) (0.3 mmol) TTD and (0.11 mmol) N-DPNQ were mixed. Then EtOH (5 ml) was added. The mixture pH was modified as 7.0 with NaOH. Finally, (0.1 mmol) $EuCl_3 \cdot 6H_2O$ and H_2O (2 ml) were poured into above EtOH solution. After reacting at 59°C (60 min), solid sample was filtered off and purified in EtOH. Elemental analysis, Found: C, 47.59; H, 2.32; N, 5.98. IR (KBr, cm^{-1}): 1598 (C=O), 464 (Eu-O). ^{1}H NMR(CDCl₃, 500 MHz) δ [ppm]: 8.55–8.59 (m, 2H), 8.45–8.49 (m, 2H), 8.21–8.24 (m, 2H), 7.82 (s, 1H), 7.59–7.56 (m, 3H), 7.42–7.45 (m, 6H), 7.12 (d, 3H), 6.28 (s, 3H), 4.44 (t, 2H), and 1.39 (t, 3H). ^{13}C NMR δ [ppm]: 172.5, 162.3, 147.6, 141.7, 140.2, 138.8, 136.9, 132.5, 128.1, 127.8, 126.5, 123.1, 121.5, 120.4, 116.6, 109.8, 89.4, 39.3, 14.1. Calculated for $C_{46}H_{27}N_5EuF_9O_6S_3$: 1164.88, MS Found: 1165.0 [M]$^{+}$.

Synthesis of Gd Reference Compounds

$Gd(N\text{-}DPNQ)_2Cl_3$: (0.07 g, 0.2 mmol) N-DPNQ was mixed with 5 ml of EtOH. Later, (0.037 g, 0.1 mmol) $GdCl_3 \cdot 6H_2O$ and ten drops of water were incorporated under stirring. The suspension was refluxed for 2 h at 80°C, and solid powder was resulted by filtration. Calculated for $C_{22}H_{23}Cl_3N_5GdO_4$: 686.0, MS Found: 686.1 [M]$^{+}$.

$Gd(TTD)_3 \cdot (H_2O)_2$: (0.067 g, 0.3 mmol) HTTD was added into 5 ml ethanol, and 1.0 mol/L 0.3 ml of NaOH was slowly incorporated. After vigorous stirring of 20 min, (0.037 g, 0.1 mmol) $GdCl_3 \cdot 6H_2O$ and ten drops of water were incorporated under stirring. The suspension was refluxed 2 h at 80°C. Solid powder was obtained by precipitating. Calculated for $C_{24}H_{16}F_9GdO_8S_3$: 856.91, MS Found: 856.9 [M]$^{+}$.

Preparation of Electrospinning Solutions

A mixed solvent 1, 2-dichloroethane/ethanol (v:v = 1:1) containing 1 g of PVP was prepared. After the solvent mixtures was stirred, a controlled amount of Eu(N-DPNQ)(TTD)₃ (0.4, 0.6, and 0.8%) relative to PVP weight was added to PVP solutions.

Electrospinning Process

When preparing the electrospinning nanofibers, the precursor solution was poured into a glass syring. Its plastic needle was wired to the anode of a high voltage generator. A plate of Al foil was placed under the plastic needle, serving as collector plat. The voltage was set as 18 kV with collecting distance between needle and collector plate of 20 cm. The current was less than 0.01 mA. The composite fibrous samples (0.4, 0.6, and 0.8%) are denoted as Eu₁, Eu₂, and Eu₃, respectively.

RESULTS AND DISCUSSION

Thermal Property

To discuss the thermal stability of Eu(N-DPNQ)(TTD)₃, its decomposition temperature is determined from TGA (thermal gravimetric analysis) curve shown in **Figure 1**. Corresponding DTG (differential thermogravimetric analysis) curve is shown for comparison as well. It is clear that Eu(N-DPNQ)(TTD)₃ is thermally stable below 300°C, and the 10% weight reduction temperature of Eu(N-DPNQ)(TTD)₃ is calculated to be 302°C. There are two regions of weight loss in the TGA curve of Eu(N-DPNQ)(TTD)₃. The first decomposition region from 300 to 358°C is attributed to release of three TTD ligands (calculated 57.3%, found 61%). Upon higher temperature of 380°C, the leaving of ligand N-DPNQ leads the gradual weight loss of Eu(N-DPNQ)(TTD)₃. There is still residual weight (19.4%) at temperature higher than 500°C. This residual weight is attributed to the remaining Eu element (13.0%) and O element (8.2%). It is assumed that Eu oxides are formed and finally preserved at the end of thermal decomposition.

Photophysical Properties

Eu(N-DPNQ)(TTD)₃ absorption, excitation, and luminescence spectra of in dichloromethane (10 μM) solutions are observed in
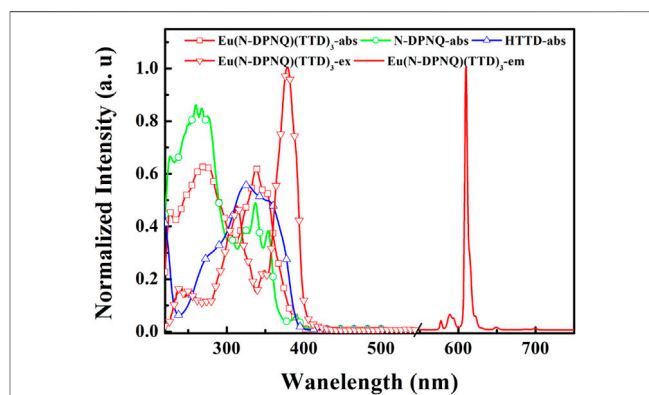

FIGURE 2 | Absorption, excitation, and PL spectra of Eu (N-DPNQ) (TTD)₃, N-DPNQ and HTTD in dichloromethane.
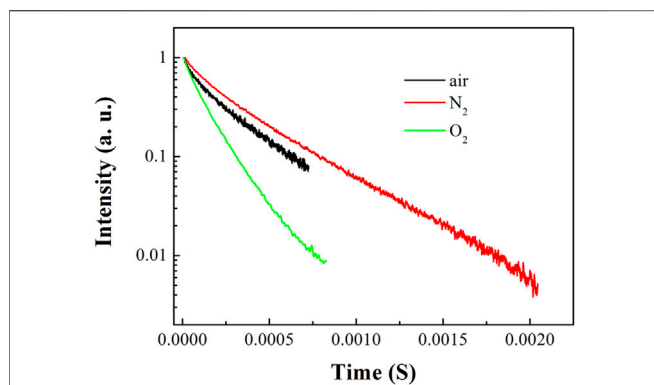
FIGURE 3 | Emission dynamics of $^5D_0-^7F_2$ transition of Eu (N-DPNQ) (TTD)$_3$ upon air, pure N$_2$ and pure O$_2$ conditions.
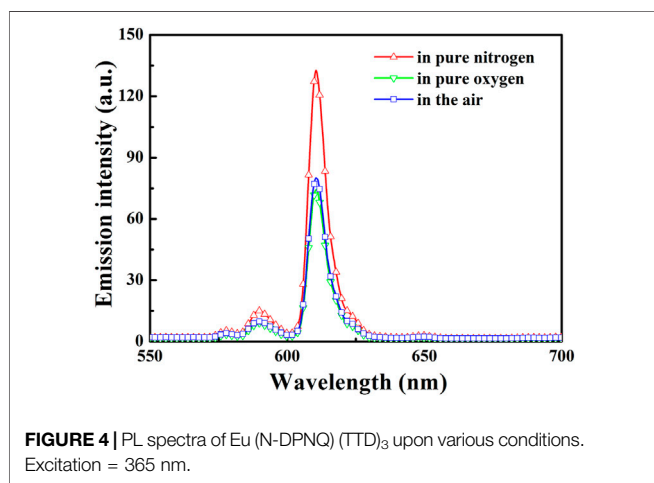

FIGURE 4 | PL spectra of Eu (N-DPNQ) (TTD)$_3$ upon various conditions. Excitation = 365 nm.

FIGURE 5 | SEM photos of Eu (N-DPNQ) (TTD)3/PVP: **(A)** Eu$_1$, **(B)** Eu$_2$, **(C)** Eu$_3$ and **(D)** a large scale view of Eu$_2$.
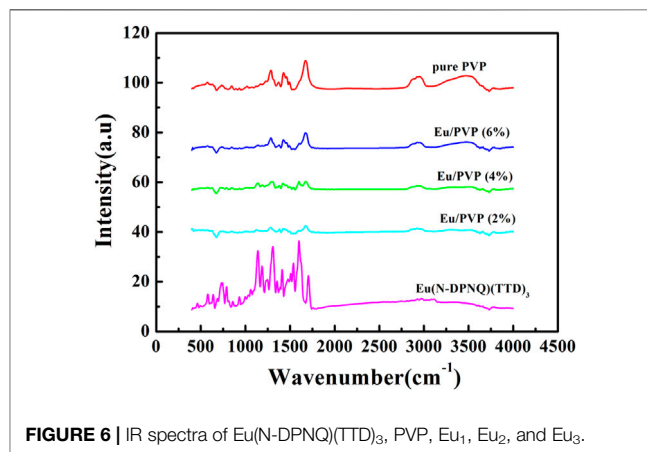
FIGURE 6 | IR spectra of Eu(N-DPNQ)(TTD)$_3$, PVP, Eu$_1$, Eu$_2$, and Eu$_3$.

Figure 2. The UV-vis absorption spectra of free N-DPNQ and free HTTD are shown in **Figure 2** as well. The absorption bands for Eu(N-DPNQ)(TTD)$_3$ locating at around 227 and 275 nm, which well matches that of N-DPNQ, are assigned as introligand π-π* electron transitions of N-DPNQ. The absorption of 339 nm corresponds to the π-π* electron transition of HTTD ligand. Eu(N-DPNQ)(TTD)$_3$ excitation bands shown in **Figure 2** are similar to its corresponding absorption spectrum. On the other hand, spectral shift and narrowed band are observed for the excitation spectra. This result suggests an indirect energy transfer dynamic from ligands to central metal ion since ligands have to experience a series of energy-wasting procedures, such as geometric relaxation, intersystem crossing and potential surface crossing, before transferring their energy to central metal ion. This statement is consistent with the antenna energy transfer procedure in rare earth complexes. The emission spectrum of Eu(N-DPNQ)(TTD)$_3$ in dichloromethane is also given in **Figure 2**. Eu(N-DPNQ)(TTD)$_3$ showed typical photoluminescence (PL) peaks of Eu(III) with five bands peaking at 578, 590, 610, 649, and 699 nm, which correspond to $^5D_0 \rightarrow {}^7F_n$ ones (n = 0–4), respectively.
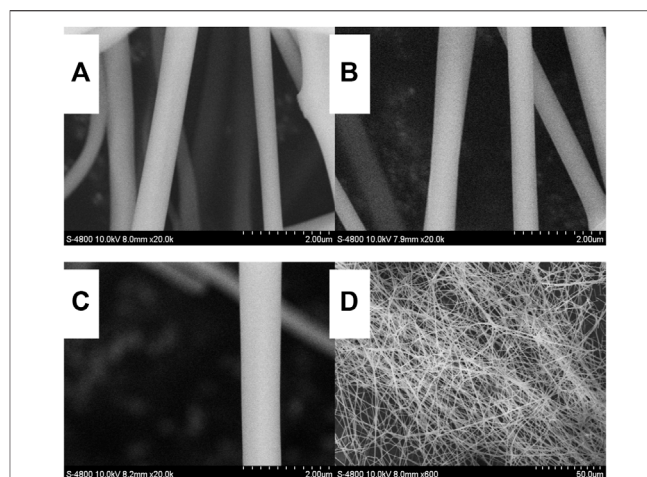
The PL quantum yield (Φ) of Eu(N-DPNQ)(TTD)$_3$ is determined with the help of a reference sample whose PL quantum yield is well determined, according to below formula.
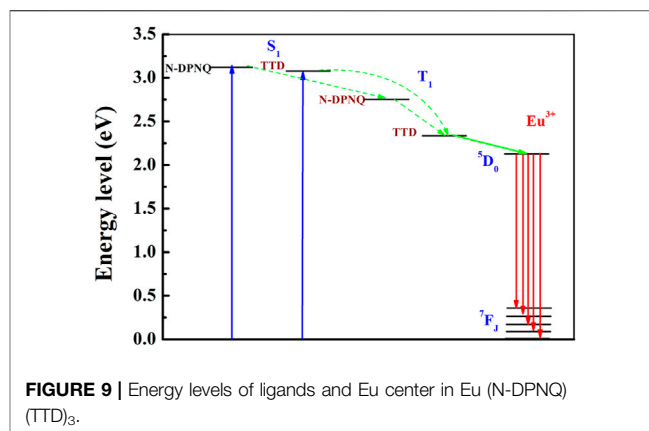
$$\Phi_{unk} = \Phi_{std} I_{unk} / A_{unk} A_{std} / I_{std} \eta_{unk}^2 / \eta_{std}^2 \qquad (1)$$

Here Φ_{unk} means Φ of unknown target. Φ_{std} =0.546 means the Φ of standard sample (Ye et al., 2005). I_{unk} and I_{std} denote the emission intensity (integrated areas) of unknown target and standard sample, respectively. A_{unk} and A_{std} indicate the absorbance of unknown target and standard sample with specific excitation position. η_{unk} and η_{std} denote solvent refractive index values of unknown target and standard sample solutions. The Φ of Eu(N-DPNQ)(TTD)$_3$ is calculated to be 0.12. The emissive dynamic decay of Eu(N-DPNQ)(TTD)$_3$ is also discussed. In **Figure 3**, Eu(N-DPNQ)(TTD)$_3$ shows a biexponential decay pattern with a mean lifetime of 268.3 µs. Corresponding two decay components are τ1 = 0.00004 s and τ2 = 0.00027 s. These two lifetime components are rather different from each other, indicating their different decay paths. Generally,

FIGURE 7 | PL spectra of Eu_1, Eu_2, and Eu_3 at different oxygen concentrations. Excitation = 365 nm.

FIGURE 9 | Energy levels of ligands and Eu center in Eu (N-DPNQ) $(TTD)_3$.

observed from **Figure 4** that the PL intensity of Eu(N-DPNQ)$(TTD)_3$ is significantly influenced by oxygen concentration. The Φ values of Eu(N-DPNQ)$(TTD)_3$ in solid state are determined as 0.18 upon 100% N_2 and 0.06 upon 100% O_2, respectively, compared to that upon air condition of 0.12. The emission intensity of $^5D_0 \rightarrow {}^7F_2$ transitions has the most obvious change among the Eu^{3+} emission lines upon 100% O_2. This observation suggests that the emission of Eu(N-DPNQ)$(TTD)_3$ complex is probably oxygen sensitive and could be applied for O_2-sensing.
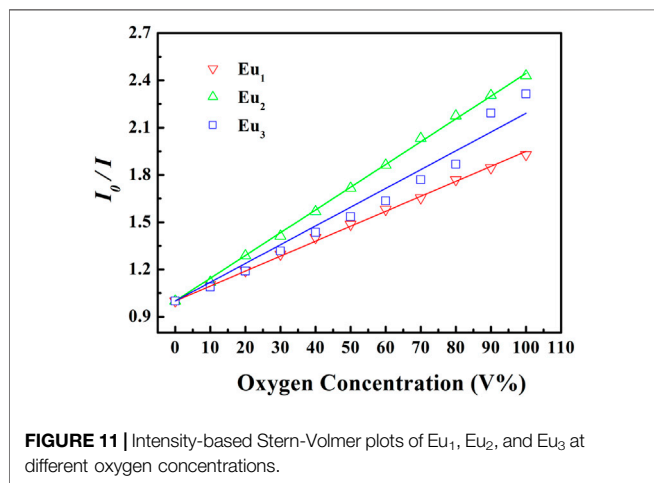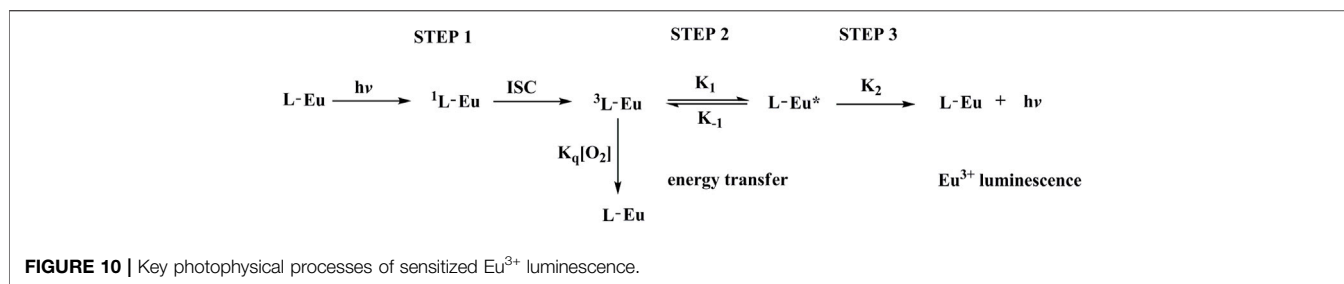
Micromorphology and Structure of Eu(N-DPNQ)$(TTD)_3$/PVP

To further realize the practical application and optimize oxygen-sensing properties, Eu(N-DPNQ)$(TTD)_3$ is incorporated in one-dimensional nanofibers of PVP. The SEM photos of all three fibrous samples are shown in **Figures 5A–D**, respectively. As shown in **Figure 5**, the uniform nanofibers have been formed through electrospinning process. The average diameters for Eu_1, Eu_2, and Eu_3 are 400, 600, and 900 nm, respectively.

Figure 6 exhibits the IR peaks of Eu(N-DPNQ)$(TTD)_3$, PVP, Eu_1, Eu_2, and Eu_3. For PVP nanofibers, the band around 1674 cm^{-1} is related with the stretching vibration of C=O. This is a characteristic band of PVP. However, this C=O band is shifted to 1665 cm^{-1} for Eu_1, Eu_2, and Eu_3. The decreased wavenumber of this C=O band is attributed to the electron-accepting effect of dopant Eu(N-DPNQ)$(TTD)_3$ on the O atom of PVP chain. This result confirms a close and direct contact between Eu(N-DPNQ)$(TTD)_3$ molecules and PVP network. In other words, dopant moleculs have been well captured by PVP host. A similar IR spectral red shift has been reported in composite samples (Zhang et al., 2008). Furthermore, the IR spectra of three fibrous samples are quite similar with that of pure PVP nanofiber, confirming that Eu(N-DPNQ)$(TTD)_3$ is well capped by PVP matrix (Zhang et al., 2007b).

Oxygen-Sensing Properties and Sensing Mechanism

To assess the oxygen-sensing ability of the composite nanofibers, the PL spectra of three fibrous samples at various O_2 levels are

FIGURE 8 | Phosphorus spectra of Gd (N-DPNQ)$_2Cl_3$ and Gd $(TTD)_3$ at 77 K.

the observation of strong absorption in UV-Vis region and a short-lived emissive center indicate a potential surface crossing procedure (Wang et al., 2002). In this case, the long-lived emissive center is attributed to the decay of Eu(III) *f-f* transitions, while the short-lived emissive center is assigned as the decay of ligand energy transfer to metal center. This assignment is consistent with its small proportion to the emissive center.

As shown in **Figure 3**, the lifetimes of Eu(N-DPNQ)$(TTD)_3$ in solid state are determined as 367.5 μs (τ1 = 0.00009 s and τ2 = 0.0004 s) upon 100% N_2 and 137.2 μs (τ1 = 0.00005 s and τ2 = 0.00015 s) upon 100% O_2, respectively, indicating an obvious oxygen quenching effect. The PL spectra of Eu(N-DPNQ)$(TTD)_3$ in solid state upon air, 100% N_2 and 100% O_2 are also measured. It is clearly

FIGURE 10 | Key photophysical processes of sensitized Eu^{3+} luminescence.

FIGURE 11 | Intensity-based Stern-Volmer plots of Eu$_1$, Eu$_2$, and Eu$_3$ at different oxygen concentrations.

TABLE 1 | Key sensing parameters for Eu$_1$, Eu$_2$, and Eu$_3$.

Loading levels (wt%)	$t_\downarrow$ (s)	$t_\uparrow$ (s)	I_0/I_{100}	K_{SV}(O$_2$%$^{-1}$)	R Nakamura et al. (2007)
Eu$_1$, 0.4	8	14	1.93	0.00949 ± 0.00007	0.998
Eu$_2$, 0.6	10	10	2.43	0.01444 ± 0.00008	0.999
Eu$_3$, 0.8	7	12	2.31	0.01191 ± 0.00039	0.969

FIGURE 12 | Response time of Eu$_1$, Eu$_2$, and Eu$_3$ upon various environmental atmospheres, emission = 610 nm.
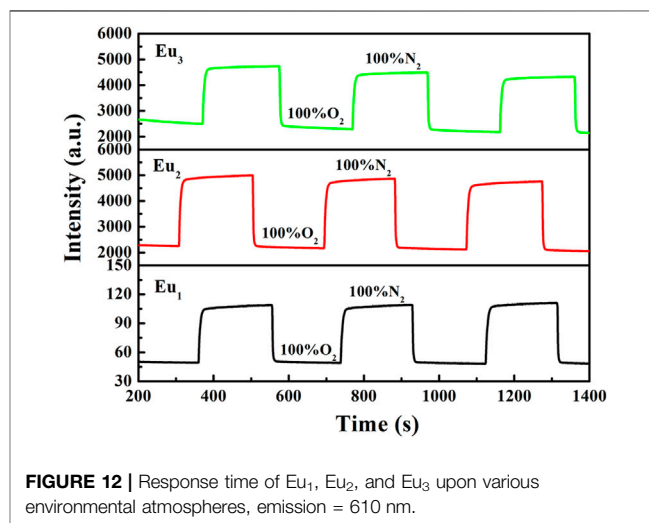
demonstrated in **Figure 7**. The PL spectra of Eu$_1$, Eu$_2$, and Eu$_3$ are similar to the PL bands of complex Eu(N-DPNQ)(TTD)$_3$, showing characteristic emissions of Eu^{3+} ion with ^{5}D$_0$→^{7}F$_n$ (n = 0–4) transitions. The emission intensity of ^{5}D$_0$→^{7}F$_2$ transition for Eu$_1$, Eu$_2$, and Eu$_3$ is quenched greatly by O$_2$.

To further investigate the quenching mechanism, energy levels of relevant electronic states of N-DPNQ and HTTD are measured. The singlet level (S$_1$) values of N-DPNQ and HTTD are measured as 3.11 eV (398 nm) and 3.08 eV (402 nm) which correspond to their absorption cutting-off values. The phosphorescence spectra of Gd(N-DPNQ)$_2$Cl$_3$ and Gd (TTD)$_3$(H$_2$O)$_2$ at 77 K are given in **Figure 8**. Correspondingly, the triplet levels (T$_1$) of Gd(N-DPNQ)$_2$Cl$_3$ and Gd (TTD)$_3$ are determined as 2.75 eV (450 nm) and 2.32 eV (533 nm).

A schematic presentation for energy transfer mechanism is shown as **Figure 9** according to above mentioned experimental results. For Eu(N-DPNQ)(TTD)$_3$, the positive energy transfer of N-DPNQ S$_1$ excited state to TTD S$_1$ excited state is difficult due to the same S$_1$ level. But partial S$_1$ energy of N-DPNQ can be transferred to N-DPNQ T$_1$ excited state. Hence such partial energy could be transferred to the lowest triplet level of TTD and then to ^{5}D$_0$ for Eu^{3+}. Furthermore, excitation energy could be transferred from TTD singlet level to TTD triplet level, and finally to ^{5}D$_0$ for Eu^{3+} (Xin et al., 2004; Xu et al., 2006). Generally, there are three main steps involved in a sensitized Eu^{3+} luminescence process, as shown in **Figure 10** (Parker, 2000). Firstly, the antenna ligand absorbs energy and is excited to its singlet level. Then this

energy is migrated to the T$_1$ excited state of antenna ligands by inter-system crossing (ISC). Next, the excitation procedure from the T$_1$ level of antenna ligands to Eu^{3+} ion excited state happens in this process. If the rate of energy transfer is sufficiently slow so as to lead a deactivation of the T$_1$ excited state of antenna ligands, the quenching by molecular oxygen could occur in this process. Finally, Eu^{3+} ion excited state energy could be transferred to the ground state, then Eu^{3+} luminescence is generated. Hence, the emission quenching of Eu^{3+} probe by molecular oxygen is based on intermolecular collision of S$_1$/T$_1$ state of antenna ligands with O$_2$ S$_0$ state. The above procedure can be presented below:

$$^*L-Eu + O_2 \rightarrow L-Eu + O_2^* \qquad (2)$$
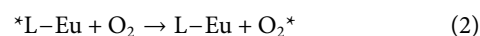
here L and Eu denote antenna ligands and Eu(III) complex, and * stands for the excited state.

The quenching of luminescent molecule in a homogeneous medium with non-obvious host afluoence is supposed to be a simple exponential dynamic procedure. The PL intensity

TABLE 2 | Sensing parameters upon different aging days.

Sample	Sensitivity/response						
	0 day	15 days	30 days	45 days	60 days	75 days	84 days
Eu_1	1.93/8	1.92/8	1.92/8	1.90/9	1.90/9	1.89/9	1.88/9
Eu_2	2.43/10	2.41/10	2.41/10	2.40/10	2.40/12	2.38/12	2.37/12
Eu_3	2.31/7	2.31/7	2.30/8	2.30/9	2.29/9	2.28/9	2.25/10

variation against O_2 levels should follow Stern-Volmer relationship.

$$\frac{I_0}{I} = \frac{\tau_0}{\tau} = 1 + K_{sv}[O_2] \qquad (3)$$

Here I and τ denote emission intensity and dynamic lifespan, respectively. I_0 is the intrinsic emission intensity with no O_2. K_{SV} shall be the Stern-Volmer constant. K_q stands for a fixed fitting parameter. $[O_2]$ means O_2 ratio. The curve of I_0/I against $[O_2]$ shall be a linear plot. Its slope shall be K_{SV}. Typical intensity-formed Stern-Volmer fitting curves for Eu_1, Eu_2, and Eu_3 are presented in **Figure 11**. These plots for Eu_1, Eu_2, and Eu_3 are well fitted by **Eq. 3**. The parameters are also found in **Table 1**. Eu_2 (with doping level of 0.6wt%) seems the optimal sample by showing the highest sensitivity of 2.43. As observed, Eu_1 and Eu_2 show a good linear relationship, whereas Eu_3 shows a poor linearity with a linearly dependent coefficient R (Nakamura et al., 2007) of 0.969. Since Eu(N-DPNQ)(TTD)$_3$ could be effectively quenched by molecular O_2, the increase in amount of Eu(N-DPNQ)(TTD)$_3$ results in increased molar fractions of oxygen-quenchable dye and hence the sensitivity and linearity of Eu_2 are superior to the corresponding values of Eu_1. If the distribution of Eu-probe in matrix is changed by increasing amount of Eu(N-DPNQ)(TTD)$_3$, this could affect the sensitivity and linearity of the sensor. In fact, the increasing of Eu(III) complex in Eu_3 leads to self-aggregation of Eu-probe molecules in the matrix, indicating that there is a change in the micro-environment of the composite nanofibers (Lee and Okura, 1997; Shi et al., 2009).

The response and recovery characteristics are very fundamental parameters for oxygen-sensing materials. Generally, response ($t_\downarrow$) and recovery ($t_\uparrow$) parameters are determined by calculating the time for each sample to lose or restore ninety five percent of maximum original emission intensity when testing atmosphere is changed between 100% N_2 and 100 O_2. **Figure 12** shows the emission variation of Eu_1, Eu_2, and Eu_3 upon surrounding atmosphere cycle of 100% N_2-100% O_2-100% N_2. Based on the dynamic variation measurements, the values of $t_\downarrow$ and $t_\uparrow$ are measured and summarized in **Table 1**. It is clear in **Figure 12** that repeatable emission responses are detected with Eu_1, Eu_2, and Eu_3. There is slice drift intensity. Furthermore, we also have monitored the mean sensitivity and response behavior of Eu_1, Eu_2, and Eu_3 over 12 weeks (interval = 15 days). The detected aging effect on sensitivity and response behavior is neglectable. The oxygen-sensing properties of Eu_1, Eu_2, and Eu_3 at 15 and 30 days also have been measured and the results are very similar, as shown in **Table 2**.

Considering the sensing mechanism of a dynamic collision between O_2 ground state and excited state probe, it is assumed that these composite nanofibers should have good sensing selectivity towards O_2 since most other gases have closed-shell structures and thus are not open for probe energy transfer. Aiming at a primitive evaluation on the sensing selectivity of these composite nanofibers, five typical interfering gases are selected, including CO_2, benzene, toluene, $CHCl_3$ and CH_2Cl_2. The emission spectra of a representative sample Eu_2 are recorded and compared in **Supplementary Figure S1** (Supporting Information). No obvious spectral shift or intensity variation is observed upon these interfering gases, which shall be attributed to the unique *f-f* transitions of these Eu(III) probes. As a consequence, it is concluded that these composite nanofibers have good selectivity for O_2. On the other hand, such *f-f* transitions needs a complicated energy transfer procedure, which makes the sensitivity far away from satisfactory. For later improvement, the antenna energy transfer from ligand to central metal ion should be simplified, so that the O_2 quenching effect on excited probe shall be efficient and complete, leading to improved sensitivity.

CONCLUSION

A Eu(III) compound have been successfully synthesized for the first time, to the best of our knowledge. Based on the quenching of luminescence for Eu(III) complex by molecular oxygen, the oxygen-sensing Eu(N-DIIQ)(TTD)$_3$/PVP composite nanofibers are prepared using electrospinning method. This work shall be extended to obtain oxygen-sensing fibrous composites having good sensitivity and linearity by altering loading levels of oxygen-sensing dye. The oxygen-sensing Eu(N-DIIQ)(TTD)$_3$/PVP composite nanofibers possess good operational stability and reproducibility. The optimized fibrous composite shows the best result with sensitivity as high as 2.43, quick response as short as 10 s and linear behavior.

DATA AVAILABILITY STATEMENT

The original contributions presented in the study are included in the article/**Supplementary Material**, further inquiries can be directed to the corresponding author.

AUTHOR CONTRIBUTIONS

CC, Writing and reviewing; LS, Data; CL, Data analysis; TL, Data; KS, Supervision. CC and LS contributed equally to this study.

FUNDING

REFERENCES

Ai, K., Zhang, B., and Lu, L. (2009). Europium-Based Fluorescence Nanoparticle Sensor for Rapid and Ultrasensitive Detection of an Anthrax Biomarker. *Angew. Chem. Int. Ed.* 48, 304–308. doi:10.1002/anie.200804231

Amao, Y., Okura, I., and Miyashita, T. (2000). Optical Oxygen Sensing Based on the Luminescence Quenching of Europium(III) Complex Immobilized in Fluoropolymer Film. *Bcsj* 73, 2663–2668. doi:10.1246/bcsj.73.2663

Amao, Y., Okura, I., and Miyashita, T. (2000). Thenoyltrifluoroacetonato 1,10-Phenanthroline Europium (III) Complex Immobilized in Fluoropolymer Film as Optical Oxygen Sensing Material. *Chem. Lett.* 29, 934–935. doi:10.1246/cl.2000.934

Baldé, C. P., C Hereijgers, B. P., Bitter, J. H., and de Jong, K. P. (2008). Sodium Alanate Nanoparticles – Linking Size To Hydrogen Storage Properties. *J. Am. Chem. Soc.* 130, 6761. doi:10.1021/ja710667v

Bauer, H., Blanc, J., and Ross, D. L. (1964). Octacoordinate Chelates of Lanthanides. Two Series of Compounds. *J. Am. Chem. Soc.* 86, 5125–5131. doi:10.1021/ja01077a016

Bian, Z.-Q., Wang, K.-Z., and Jin, L.-P. (2002). Syntheses, Spectroscopic and crystal Structural Studies of Novel Imidazo[4,5-F]1,10-Phenanthroline Derivatives and Their Eu(III) Ternary Complexes with Dibenzoylmethane. *Polyhedron* 21, 313–319. doi:10.1016/s0277-5387(01)00995-0

Bodige, S., and MacDonnell, F. M. (1997). Synthesis of Free and Ruthenium Coordinated 5,6-Diamino-1,10-Phenanthroline. *Tetrahedron Lett.* 38, 8159–8160. doi:10.1016/s0040-4039(97)10223-4

Bolger, J., Gourdon, A., Ishow, E., and Launay, J.-P. (1996). Mononuclear and Binuclear Tetrapyrido[3,2-A:2',3'-C:3",2"-H:2"',3"'-J]phenazine (Tpphz) Ruthenium and Osmium Complexes. *Inorg. Chem.* 35, 2937–2944. doi:10.1021/ic951436w

Dodiuk-kenig, h., Lizenboim, K., Roth, S., Zalsman, B., McHale, W. A., Jaffe, M., et al. (2008). Performance Enhancement of Dental Composites Using Electrospun Nanofibers. *J. Nanomater.* 2008, 1. doi:10.1155/2008/840254

Greiner, A., and Wendorff, J. H. (2007). Electrospinning: A Fascinating Method for the Preparation of Ultrathin Fibers. *Angew. Chem. Int. Ed.* 46, 5670–5703. doi:10.1002/anie.200604646

Gunnlaugsson, T., Leonard, J. P., Sénéchal, K., and Harte, A. J. (2004). Eu(Iii)–Cyclen–Phen Conjugate As A Luminescent Copper Sensor: The Formation Of Mixed Polymetallic Macrocyclic Complexes In Water. *Chem. Commun.* 7, 782. doi:10.1039/b316176e

Gunnlaugsson, T., Leonard, J. P., Sénéchal, K., and Harte, A. J. (2003). pH Responsive Eu(III)–Phenanthroline Supramolecular Conjugate: Novel "Off–On–Off" Luminescent Signaling in the Physiological pH Range. *J. Am. Chem. Soc.* 125, 12062–12063. doi:10.1021/ja035425a

Huang, Z.-M., Zhang, Y.-Z., Kotaki, M., and Ramakrishna, S. (2003). A Review on Polymer Nanofibers by Electrospinning and Their Applications in Nanocomposites. *Composites Sci. Techn.* 63, 2223–2253. doi:10.1016/s0266-3538(03)00178-7

Lee, S.-K., and Okura, I. (1997). Optical Sensor for Oxygen Using a Porphyrin-Doped Sol-Gel Glass. *Analyst* 122, 81–84. doi:10.1039/a604885d

Li Kong, L., Yan, B., and Li, Y. (2009). Mesoporous Hybrids Containing Eu3+ Complexes Covalently Bonded to SBA-15 Functionalized: Assembly, Characterization and Photoluminescence. *J. Solid State. Chem.* 182, 1631–1637. doi:10.1016/j.jssc.2009.03.036

Li, S., Song, H., Li, W., Ren, X., Lu, S., Pan, G., et al. (2006). Improved Photoluminescence Properties of Ternary Terbium Complexes in Mesoporous Molecule Sieves. *J. Phys. Chem. B* 110, 23164–23169. doi:10.1021/jp064509d

Li, Y., and Yan, B. (2008). Hybrid Materials of MCM-41 Functionalized by Lanthanide (Tb3+, Eu3+) Complexes of Modified Meta-Methylbenzoic

Acid: Covalently Bonded Assembly and Photoluminescence. *J. Solid State. Chem.* 181, 1032–1039. doi:10.1016/j.jssc.2008.02.001

Liu, Q., Li, B., Gong, J., Sun, Y., and Li, W. (2008). Preparation and Luminescent Properties of One-Dimensional [Ru(Bphen)2dppz]Cl2/PVP Composite Fibers by Electrospinning. *J. Alloys Comp.* 466, 314–318. doi:10.1016/j.jallcom.2007.11.048

Nakamura, K., Hasegawa, Y., Kawai, H., Yasuda, N., Kanehisa, N., Kai, Y., et al. (2007). Enhanced Lasing Properties of Dissymmetric Eu(III) Complex with Bidentate Phosphine Ligands. *J. Phys. Chem. A.* 111, 3029–3037. doi:10.1021/jp067672h

Park, J.-Y., Suh, M., and Kwon, Y.-U. (2010). Humidity Sensing by Luminescence of Eu(III)-doped Mesoporous Silica Thin Film. *Microporous Mesoporous Mater.* 127, 147–151. doi:10.1016/j.micromeso.2009.07.008

Parker, D. (2000). Luminescent Lanthanide Sensors for pH, pO2 and Selected Anions. *Coord. Chem. Rev.* 205, 109–130. doi:10.1016/s0010-8545(00)00241-1

Shi, L., Li, B., Yue, S., and Fan, D. (2009). Synthesis, Photophysical and Oxygen-Sensing Properties of a Novel Bluish-green Emission Cu(I) Complex. *Sensors Actuators B: Chem.* 137, 386–392. doi:10.1016/j.snb.2008.12.039

Sun, P.-P., Duan, J.-P., Shih, H.-T., and Cheng, C.-H. (2002). Europium Complex as a Highly Efficient Red Emitter in Electroluminescent Devices. *Appl. Phys. Lett.* 81, 792–794. doi:10.1063/1.1497714

Sun, P. P., Duan, J. P., Lih, J. J., and Cheng, C. H. (2003). Synthesis of New Europium Complexes and Their Application in Electroluminescent Devices. *Adv. Funct. Mater.* 13, 683–691. doi:10.1002/adfm.200304378

Takahashi, Y., Danwittayakul, S., and Suzuki, T. M. (2009). Dithizone Nanofiber-Coated Membrane for Filtration-Enrichment and Colorimetric Detection of Trace Hg(ii) Ion. *Analyst* 134, 1380. doi:10.1039/b816461d

Tan, S., Feng, X., Zhao, B., Zou, Y., and Huang, X. (2008). Preparation and Photoluminescence Properties of Electrospun Nanofibers Containing PMO-PPV and Eu(ODBM)3phen. *Mater. Lett.* 62, 2419–2421. doi:10.1016/j.matlet.2007.12.036

Wang, F., Wang, W., Liu, B., Wang, Z., and Zhang, Z. (2009). Copolypeptide-doped Polyaniline Nanofibers for Electrochemical Detection of Ultratrace Trinitrotoluene. *Talanta* 79, 376–382. doi:10.1016/j.talanta.2009.03.062

Wang, W., Zhang, L., Tong, S., Li, X., and Song, W. (2009). Three-dimensional Network Films of Electrospun Copper Oxide Nanofibers for Glucose Determination. *Biosens. Bioelectron.* 25, 708–714. doi:10.1016/j.bios.2009.08.013

Wang, X., Drew, C., Lee, S.-H., Senecal, K. J., Kumar, J., and Samuelson, L. A. (2002). Electrospun Nanofibrous Membranes for Highly Sensitive Optical Sensors. *Nano Lett.* 2, 1273–1275. doi:10.1021/nl020216u

Wang, Y., Li, B., Liu, Y., Zhang, L., Zuo, Q., Shi, L., et al. (2009). Highly Sensitive Oxygen Sensors Based on Cu(i) Complex-Polystyrene Composite Nanofibrous Membranes Prepared by Electrospinning. *Chem. Commun.* 39, 5868. doi:10.1039/b910305h

Xin, H., Shi, M., Gao, X. C., Huang, Y. Y., Gong, Z. L., Nie, D. B., et al. (2004). The Effect of Different Neutral Ligands on Photoluminescence and Electroluminescence Properties of Ternary Terbium Complexes. *J. Phys. Chem. B* 108, 10796–10800. doi:10.1021/jp037816h

Xu, H., Wang, L.-H., Zhu, X.-H., Yin, K., Zhong, G.-Y., Hou, X.-Y., et al. (2006). Application of Chelate Phosphine Oxide Ligand in EuIII Complex with Mezzo Triplet Energy Level, Highly Efficient Photoluminescent, and Electroluminescent Performances. *J. Phys. Chem. B* 110, 3023–3029. doi:10.1021/jp055355p

Xu, Q., Li, L., Liu, X., and Xu, R. (2002). Incorporation of Rare-Earth Complex Eu(TTA)4C5H5NC16H33 into Surface-Modified Si–MCM-41 and its Photophysical Properties. *Chem. Mater.* 14, 549–555. doi:10.1021/cm0102234

Yan, B., and Wang, Q.-M. (2008). Two Luminescent Molecular Hybrids Composed of Bridged Eu(III)-β-Diketone Chelates Covalently Trapped in Silica and Titanate Gels. *Cryst. Growth Des.* 8, 1484–1489. doi:10.1021/cg0603725

SUPPLEMENTARY MATERIAL

The Supplementary Material for this article can be found online at: https://www.frontiersin.org/articles/10.3389/fchem.2021.812461/full#supplementary-material

Ye, K., Wang, J., Sun, H., Liu, Y., Mu, Z., Li, F., et al. (2005). Supramolecular Structures and Assembly and Luminescent Properties of Quinacridone Derivatives. *J. Phys. Chem. B* 109, 8008–8016. doi:10.1021/jp0444767

Zhang, H., Song, H., Dong, B., Han, L., Pan, G., Bai, X., et al. (2008). Electrospinning Preparation and Luminescence Properties of Europium Complex/Polymer Composite Fibers. *J. Phys. Chem. C* 112, 9155–9162. doi:10.1021/jp7115005

Zhang, H., Song, H. W., Yu, H. Q., Bai, X., Li, S. W., Pan, G. H., et al. (2007). Electrospinning Preparation And Photoluminescence Properties Of Rare-Earth Complex/Polymer Composite Fibers. *J. Phys. Chem. C.* 111, 6524. doi:10.1021/jp0684123

Zhang, H., Song, H., Yu, H., Li, S., Bai, X., Pan, G., et al. (2007). Modified Photoluminescence Properties of Rare-Earth Complex/polymer Composite Fibers Prepared by Electrospinning. *Appl. Phys. Lett.* 90, 103103. doi:10.1063/1.2711380

Zhang, L., Li, B., Su, Z., and Yue, S. (2010). Novel rare-Earth(III)-based Water Soluble Emitters for Fe(III) Detection. *Sensors Actuators B: Chem.* 143, 595–599. doi:10.1016/j.snb.2009.09.056

Zhang, L., Li, B., Zhang, L., Chen, P., and Liu, S. (2009). Synthesis, Characterization, and Luminescent Properties of Europium Complexes with Fluorine Functionalized Phenanthroline. *J. Electrochem. Soc.* 156, H202. doi:10.1149/1.3060228

Zuo, Q., Li, B., Zhang, L., Wang, Y., Liu, Y., Zhang, J., et al. (2010). Synthesis, Photophysical and Oxygen-Sensing Properties of a Novel Eu3+ Complex Incorporated in Mesoporous MCM-41. *J. Solid State. Chem.* 183, 1715–1720. doi:10.1016/j.jssc.2010.05.022